Implementation of FPGA based three-level converter for LED drive applications

J. GNANAVADIVEL*, N. SENTHIL KUMAR, P. YOGALAKSHMI
Electrical and Electronics Engineering Department, Mepco Schlenk Engineering College, Sivakasi, Tamilnadu, India

A fuzzy-tuned PI voltage controller and a hysteresis current controller operating a single-phase AC-DC three-level converter is proposed for improving power quality at AC mains for LED drive applications. A prototype of 100 W, 48 V LED driver is considered for the testing of controller performance. Performance parameters such as input power factor and input current total harmonic distortion (THD) are considered. Three-level LED driver with voltage and current controller combinations such as PI-Hysteresis, Fuzzy-Hysteresis and Fuzzy tuned PI-Hysteresis are carried out in MATLAB platform. The proposed combination with the three-level LED driver provides a better result, with a source-current THD of 1.24% and a unity power factor without any source side filter. Finally, the proposed controller combination is implemented in a Xilinx Spartan-6 XC6SLX25 FPGA board for experimental validation of power quality improvement in proposed LED drive.

(Received December 23, 2015; accepted June 09, 2016)

Keywords: Fuzzy-Tuned PI voltage controller, Hysteresis Current Controller, Input Power Factor, Total Harmonic Distortion (THD), Three-Level LED drive

1. Introduction

Nowadays, light emitting diode lamps are very popular to be used in many applications, for example inside and outside of the residence, offices, street lighting, industrial lighting, building decoration and vehicle applications. With the development of lighting technology in past few years, high luminance LED are used as source of artificial light because of their own merits like high luminous efficiency, long life, low power consumption, environment friendly because there is less mercury contents, easily dimmable, low maintenance, flicker less start, robust in structure and least affected by vibrations[1]-[6]. LED lighting module consists of two major parts: LED driver and LED module. Even though LED lamp has many merits, it also has some demerits such as generation of harmonics in the input AC side and low input power factor because of switching devices of the LED driver. Most of the research papers are focused on development of LED lamps, lighting control and illumination on the work surface [7] - [12]. But some of the research papers are focusing on the power quality of the input side of the LED lamp driver.

Diode-based rectifiers are a widely used power supply for driving LED lamps. The major disadvantages of the conventional diode and thyristor-based rectifiers are low input power factor and high input current harmonics in the AC supply. These drawbacks can be rectified by adding inductor and capacitor at input side [13]. Inserting an inductor on the AC supply side is a simple method for improving the input current waveform but this solution reduces the input power factor [14]. A passive wave shaping method can be used to lower rectifier current stresses and improve the power factor [15]. IEEE 516 and IEC 61000-3-2 standards prescribe the allowable limit of harmonics on the input side power quality [16], [17]. With the ever-increasing use of power electronic products, power factor correction (PFC) has become more become important. With this in mind, reduced-size low-cost high-efficiency power converters are the best choice [18]. An input PFC function includes shaping the input current waveform and regulating the output voltage. Due to the need for continuous input current, boost-type converters have been widely integrated into AC-DC converters for driving LED lamps to achieve the derived PFC function and harmonic reduction [19]. Accurate mode boundary detection is performed by using accurate inductance estimated as a result of the tuning process; this estimate can be useful for a digital current programmed control technique [20]. The output voltage is sensed for the outer loop to regulate the derived output. Sensing the input voltage is also required for the generation of the derived current reference and the feed forward terms [21]. A feed-forward control is significantly helpful for the control action needed for performance sensitivity to parameter variations and uncertainties [22]. Some compensation loops are added to the multi-loop control to improve the PFC performance for motor drive applications in order to regulate the speed of a motor. As for the boost converter, the single switch needs to withstand the overall output voltage when the switch blocks the signal. To overcome this, multi-level AC-DC converters are used for high-voltage, high-power applications where power semiconductors devices with high-voltage stress are generally required [23]. Randomly varying the band hysteresis with current-controlled pulse width modulation schemes are adopted for acoustic noise reduction using a switch mode rectifier for the PMSM drive [24].

To achieve high step-up voltage, gain-coupled inductors and voltage doubler circuits are integrated in the

DC-DC converter [25]. A conventional single-phase three-level AC-DC requires eight switches, which is a drawback of the system. Therefore, a single-phase AC-DC multilevel converter that requires only two power semiconductor switches is used [26]. Two capacitors are connected across the switches with a three-level boost converter. Thus, each switch must withstand only half the output voltage. In addition, the inductor current ripple in the three-level boost converter is lower than that of those obtained in a conventional boost converter because there are three levels of inductor voltage in the three-level AC-DC converter. As a result, three-level converters are often used in high-voltage ratio DC-DC conversion applications, particularly in fuel cell applications [27]. Fuel cell applications involving DC-DC converters with wide input range three-level converters are also used [28]. A three-level boosting MPPT control is used in photovoltaic systems to reduce recovery losses of diodes in order to increase power conversion efficiency [29].

Multi-level AC-DC converters are the most preferable choice for wind energy systems to reduce the cost, size and complexity of the systems compared to two-level boost converters [30]. In addition, high withstanding voltage semiconductor switches often have larger drain-source resistances. Thus, three-level converters possess the advantages of low voltage stress, low inductor current ripple and low switching loss [31]. A synchronized PWM, as implemented in a three-level data rectifier, has a reduced input current ripple with low input current THD [32]. Voltage compensators with three-level PWM control schemes are used to provide better capacitor voltage balance in multi-level AC-DC converters [33]. A hysteresis current control, adopted with a power estimates and voltage compensator block, improve the input power quality with a input current THD of 6% [34]. A multi-loop interleaved control with reduced sensing parameters is implemented for the improved input power quality and operation of the three-level AC-DC converter [35].

Midpoint converter SRM performance is improved by the use of a single-phase three-level AC-DC converter and to improve power quality at the AC supply side [36]. Boost power factor correction converters are used to drive high-brightness LEDs with high power factor and source current THD is 10.72% [37]. Boost converter topology is used to drive the LED with film capacitor and input power factor is 0.99 and source current THD is 10% [38]. A full bridge diode rectifier and a quasi-resonant flyback converter are used to drive LED. For this configuration, the input power factor is 0.988 and the harmonics are in compliance with IEC61000-3-2 Class D [39]. A diode bridge rectifier with flyback based ripple cancellation converter is used to drive LED with no flicker and high power factor of 0.99 [40]. A comparative study of PI, fuzzy and ANN controllers is made for the speed control of the DC motor fed by a Buck-type DC-DC converter [41]. A DC motor possessing non-linearity can be controlled and regulated through the proper design methods of a fuzzy logic controller [42]. The DC bus voltage at the required level can be maintained by using a PI as well as a fuzzy logic controller. Good performance is achieved during transient states while using a fuzzy logic controller. Fuzzy logic controllers are applicable in DC-DC converters as well as two-level AC-DC converters [43],[44]. Self tuning of fuzzy PI controllers is used in various DC-DC converters for the optimization of errors and reactive power control [45]-[49].

This paper proposes a self tuning of fuzzy PI voltage control and hysteresis current control for a single-phase three-level AC-DC LED driver circuit. PI voltage controller with a hysteresis current controller, fuzzy logic voltage controller with a hysteresis current controller and a self tuning of fuzzy PI voltage controller with a hysteresis current controller are implemented for the LED driver with the objective of drawing a pure sinusoidal input current with low total current harmonic distortion and high input power factor. The performance of the proposed fuzzy-tuned PI control method is also compared with the PI and fuzzy logic control methods. The three level AC-DC converter can be used as front stages for LED drive applications.

2. Modeling of AC-DC three-level LED driver

Fig. 1 shows the single-phase AC-DC three-level LED driver. This driver circuit topology consists of a single-phase diode bridge rectifier, two power switching devices, one inductor, two fast-recovery diodes and two DC capacitors. An inductor L_b is used to reduce inductor current ripple. The voltage rating of the power semiconductor switches are reduced to half of the DC bus voltage. The single-phase three-level LED driver can be analyzed in its four operating modes according to the states of two power semiconductor switches Sw_1 and Sw_2.

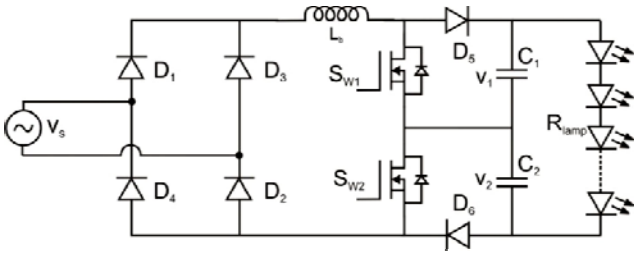

Fig. 1. Circuit configuration of single-phase AC-DC three-level LED driver

Based on the LED driver circuit diagram, when Sw_1 and Sw_2 are ON, the modeling equations are

$$\left|v_s\right| = L_b \frac{di_L}{dt} \tag{1a}$$

$$C_1 \frac{dv_1}{dt} = - \frac{v_d}{R_{lamp}} \tag{1b}$$

$$C_2 \frac{dv_2}{dt} = - \frac{v_d}{R_{lamp}} \tag{1c}$$

Based on the LED driver circuit diagram, when Sw_1 ON and Sw_2 are OFF, the modeling equations are

$$L_b \frac{di_L}{dt} = v_s - \frac{v_d}{2} \tag{2a}$$

$$C_1 \frac{dv_1}{dt} = -\frac{v_d}{R_{lamp}} \tag{2b}$$

$$C_2 \frac{dv_2}{dt} = i_L - \frac{v_d}{R_{lamp}} \tag{2c}$$

Based on the LED driver circuit diagram, when Sw_1 is OFF and Sw_2 is ON, the modeling equations are

$$L_b \frac{di_L}{dt} = v_s - \frac{v_d}{2} \tag{3a}$$

$$C_1 \frac{dv_1}{dt} = i_L - \frac{v_d}{R_{lamp}} \tag{3b}$$

$$C_2 \frac{dv_2}{dt} = -\frac{v_d}{R_{lamp}} \tag{3c}$$

Based on the LED driver circuit diagram, when Sw_1 and Sw_2 are OFF, the modeling equations are

$$L_b \frac{di_L}{dt} = v_s - v_d \tag{4a}$$

$$C_1 \frac{dv_1}{dt} = i_L - \frac{v_d}{R_{lamp}} \tag{4b}$$

$$C_2 \frac{dv_2}{dt} = i_L - \frac{v_d}{R_{lamp}} \tag{4c}$$

2.1 Design of the proposed LED Driver

The following considerations are made to design the proposed LED driver.

- All the circuit components of proposed LED driver are considered ideal.
- Under steady state condition, LED behaves as a pure resistor.

The boost inductor:

$$L_b = -\frac{V_d}{4 f_{sw} \Delta I} \tag{5}$$

where V_d is the output voltage,

ΔI is the inductor current ripple (1% of inductor current)

f_{sw} is the switching frequency.

DC link capacitors:

$$C_1 = C_2 = \frac{I_d}{2\omega \Delta V_1} \tag{6}$$

where ΔV_1 is the ripple voltage across the capacitor (2% of individual capacitor voltage)

ω is the angular frequency of the supply voltage and

I_d is the lamp load current.

Table 1 shows the design specifications and circuit parameters of the proposed LED driver.

Table 1. Design specifications and circuit parameters

S. No	Parameter	Specification
1	Input supply voltage (V_s)	28 V
2	LED lamp voltage (V_d)	48 V
3	LED lamp load power (P_o)	100 W
4	LED driver Switching frequency (f_{sw})	10 kHz
5	Line frequency (f_s)	50 Hz
6	Boost inductor (L_b)	3 mH
7	Output Capacitance C_1=C_2	7000 µF
8	LED lamp load resistance (R_{lamp})	23Ω

3. Design of controllers for proposed LED driver

The proposed block diagram of the single-phase AC-DC three-level LED driver is shown in Fig 2. It consists of a three-level AC-DC LED driver, a voltage controller, a phase-locked loop and a current controller. The LED driver output voltage is sensed and compared with the reference voltage. After comparison of these two signals, an error signal is fed to the voltage controller. The input voltage is processed by the phase-locked loop in order to produce an absolute value of sinωt. The voltage controller output and the absolute value of sinωt are multiplied and used to obtain the amplitude of the reference inductor current. This reference inductor current is compared with the actual inductor current and this error signal is fed to the inner hysteresis current control loop. This hysteresis current controller generates one control signal that controls the switching times of switch Sw_1, and a delay is introduced to the current controller output that controls the switching times of switch Sw_1.

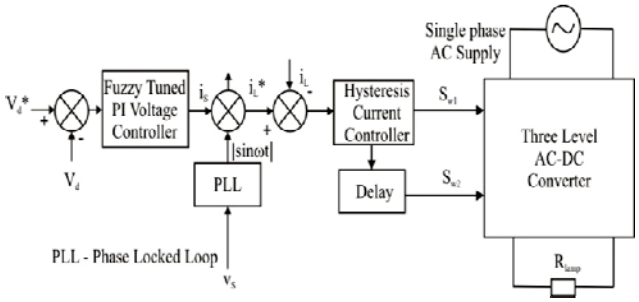

Fig. 2. Proposed block diagram of single-phase AC-DC three-level LED driver

3.1 Fuzzy-tuned PI voltage controller for LED driver

In this paper, the implementation of a fuzzy-tuned PI controller in a three-level boost-type LED driver affords power quality improvement in both the source side and output voltage regulation. Fig. 3 shows the structure of fuzzy tuned PI controller for the proposed LED driver. The fuzzy tuned PI controller is used to regulate the DC output voltage of the LED driver, where the gain of the controller is adjusted adaptively. The proposed control algorithm effectively improves the input power quality by reducing the total harmonic distortion of the input current and simultaneously adjusting the input power factor to near unity. Fuzzy tuned PI controllers have self-tuning ability and can adapt on line to nonlinear, time varying and indecisive systems. Fuzzy tuned PI controllers provide a promising option for industrial LED lighting system.

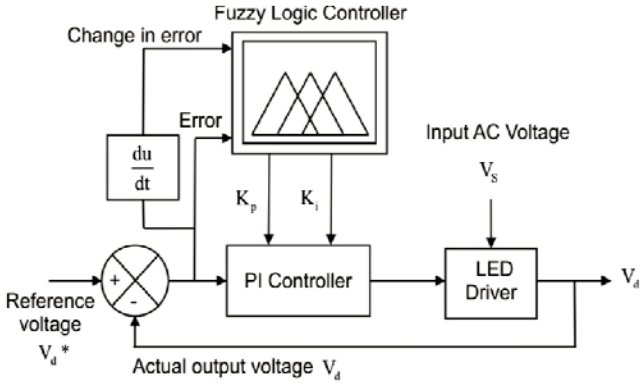

Fig. 3. Structure of fuzzy-tuned PI controller for LED driver

This fuzzy controller can be integrated with the conventional PI control for the self tuning of controller gains of the PI controller for proposed LED driver, as shown in Fig 3. The error and error differentiation signals are then fed into the fuzzy logic controller, which then produces the outputs as K_p and K_i by using a fuzzy logic inference system that operates based on rule-based membership functions. Instead of deriving a perfect mathematical model of the working converter and tuning the gain parameters (as is the usual procedure in conventional PI controller), this fuzzy-tuned PI easily tunes the gain parameters without any mathematical modeling of the converter.

Table 2 shows the decision matrix for the proportional gain of the PI controller depending upon the error and change in error for proposed LED driver. This table is called a fuzzy associative memory table. It will be chosen based upon the operational characteristics of the system.

Table 2. Decision matrix for K_P

CE / E	NB	NM	NS	ZE	PS	PM	PB
NB	NB	NB	NB	NB	NM	NS	ZE
NM	NB	NB	NB	NM	NS	ZE	PS
NS	NB	NB	NM	NS	ZE	PS	PM
ZE	NB	NM	NS	ZE	PS	PM	PB
PS	NM	NS	ZE	PS	PM	PB	PB
PM	NS	ZE	PS	PM	PB	PB	PB
PB	ZE	PS	PM	PM	PB	PB	PB

Table 3 shows the fuzzy associative memory table for the selection of the optimal integral gain of the PI controller depending on inputs such as error and change in error of the proposed LED driver.

Table 3. Decision matrix for K_i

CE / E	NB	NM	NS	ZE	PS	PM	PB
NB	NB	NB	NB	NM	NM	NS	ZE
NM	NB	NB	NM	NM	NS	ZE	PS
NS	NB	NM	NM	NS	ZE	PS	PM
ZE	NM	NM	NS	ZE	PS	PM	PM
PS	NM	NS	ZE	PS	PM	PM	PB
PM	NS	ZE	PS	PM	PM	PB	PB
PB	ZE	PS	PM	PM	PB	PB	PB

These tables are produce the desired output based upon the given inputs with the help of the rule base in a fuzzy inference system. Thus, for every variation in load or source parameters, K_p and K_i for the proportional controller will be reorganized in correspondence to the changes in input and output parameters.

3.2 Design of Hysteresis current controller for LED driver

A hysteresis current controller is used with a closed-loop control system of proposed LED drive applications. An error signal e(t) is used to inspect the switches in the LED driver. This error is the difference between the desired current i_{ref} and the current through the boost inductor i_{act}. When the error reaches an upper limit, the power MOSFET is switched to lower the current. When the error reaches at a lower limit, the current is forced to ascend. The turn-on and turn-off conditions for LED driver switch using hysteresis band are as follows:

- Switch will be Off: if ($i_{ref} - i_{act}$) > Hysteresis band
- Switch will be On: if ($i_{ref} - i_{act}$) < - Hysteresis band

This hysteresis current controller shapes the input current to be pure sinusoidal and reduces the harmonic distortions present in the input current. An appropriate bandwidth must be selected in correspondence with the switching capability of the LED driver. The fixed hysteresis band is very straightforward and easy to accomplish. In this proposed LED driver, the hysteresis band value is 0.1.

4. Simulation results and analysis of the three level LED driver

The PI voltage outer loop controller with Hysteresis current inner loop controller, the fuzzy logic voltage outer loop controller with hysteresis current inner loop controller and the proposed fuzzy based tuned PI voltage outer loop controller with hysteresis current control methods are simulated through MATLAB Simulink platform for proposed LED driver.

4.1 Simulation results with proposed fuzzy-tuned PI voltage controller and hysteresis current controller for LED driver

Fig. 4 shows simulated circuit diagram of fuzzy tuned PI voltage controller and hysteresis current controller for LED driver. In this closed loop system, the fuzzy-tuned PI controller is used for output voltage regulation and the hysteresis controller is used for input current control for shaping the source current waveform. The performance analysis shows better results for this proposed topology of controller combinations in a three-level AC–DC LED driver.

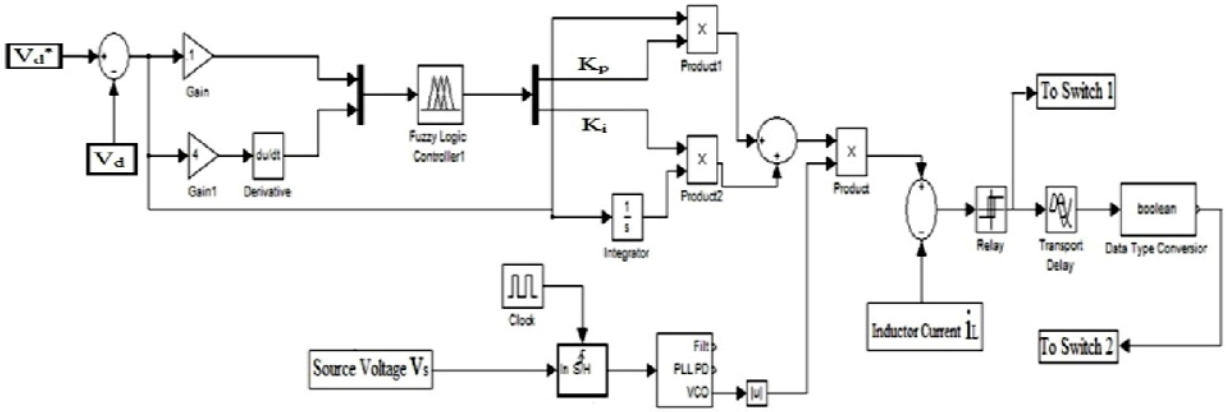

Fig. 4. Simulated circuit diagram of fuzzy-tuned PI voltage controller and hysteresis current controller for LED driver.

Fig. 5 shows the input voltage and input current waveforms for the fuzzy-tuned PI voltage controller and the hysteresis current controller for LED driver. The input current waveform is purely sinusoidal.

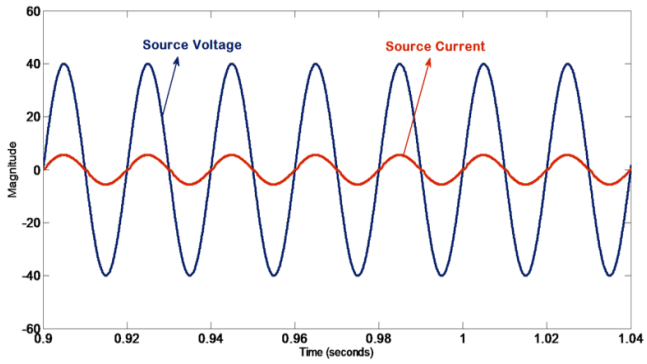

Fig. 5. Input voltage and input current waveforms for fuzzy-tuned PI voltage controller and hysteresis current controller for LED driver

Fig. 6 shows the FFT analysis for the fuzzy tuned PI voltage controller and the hysteresis current controller for LED driver. The input current total harmonic distortion is very low at 1.24%.

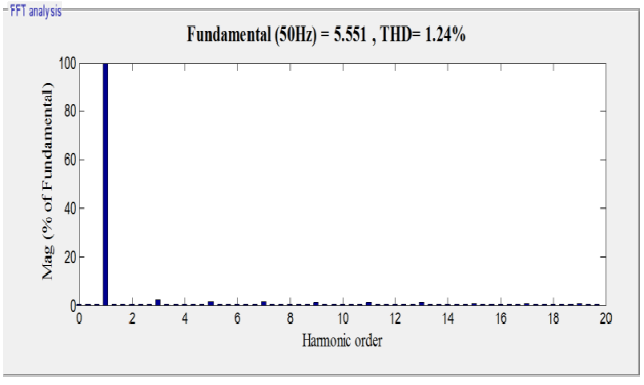

Fig. 6. FFT analysis for fuzzy-tuned PI voltage controller and hysteresis current controller for LED driver.

Fig.7 shows the desired output voltage waveform 48V for the fuzzy tuned PI voltage controller and the hysteresis current controller for LED lamp load.

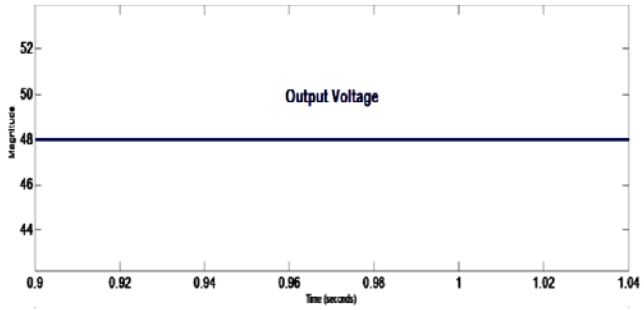

Fig. 7. Output voltage waveform of fuzzy-tuned PI voltage controller and hysteresis current controller for LED driver.

Table 4 shows the performance analysis of the three-level LED driver for the fuzzy-tuned PI voltage controller and the hysteresis current controller for various lamp load power. The output voltage is maintained at 48 V for various lamp load. By implementing this control method produces input power factor very close to unity and a very low value of input current THD at 1.24%.

Table 4. Performance analysis of three – level LED driver for fuzzy tuned PI voltage controller and hysteresis current controller

LED Lamp Load (%)	Output Voltage (V)	Input Current THD (%)	Input Power Factor	Input Current (A)
100	48	1.24	1	3.97
75	48	1.58	1	2.94
50	48	1.73	1	1.96
25	48	2.02	1	0.98

5. FPGA implementation of proposed LED driver

Fig. 8 shows the proposed hardware setup system for LED driver. The fuzzy tuned PI and hysteresis controller implemented using VHDL language on a Xilinx Spartan-6 XC6SLX25 FPGA board. The output voltage V_d, the inductor currents i_L and the source voltage V_s are sensed from the circuit and assigned to ADC as an input. These converted digital signals are given to the FPGA-based control board. Based on the control algorithm, the FPGA generates two gating signals. These gating signals are fed to the single-phase three-level LED driver.

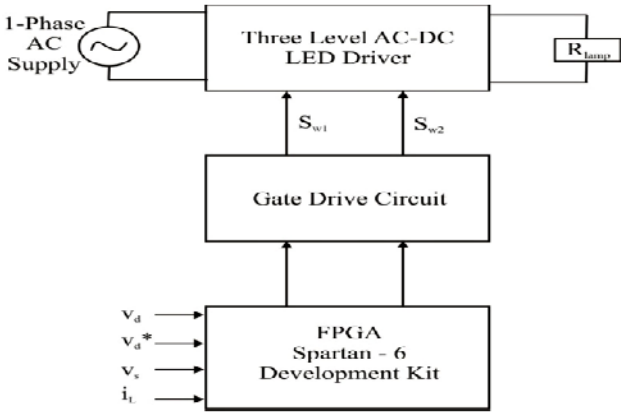

Fig. 8. Block Diagram of Hardware setup.

5.1 Experimental results of proposed LED driver

To verify the validity of the proposed fuzzy-tuned PI voltage controller and hysteresis current controller, a single-phase three-level LED driver has been built and tested in the laboratory. It is shown fig. 9.

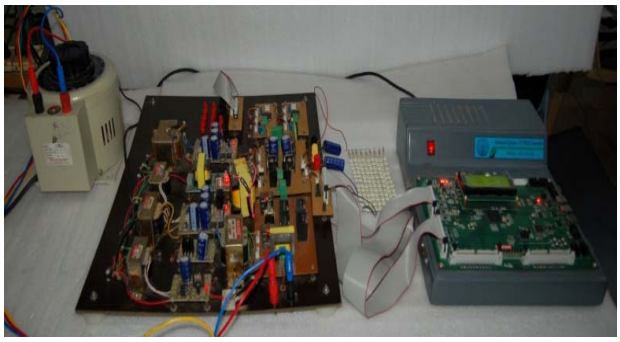

Fig. 9. Hardware setup of proposed LED driver

The power switching devices and various components of the prototype include an MUR360 input rectifier bridge, IRF250 power Mosfet switches, a 3mH boost inductor, a 7000 µF output filter capacitor, an FPGA Spartan-6 controller, an HCPL-7840 voltage sensor, a WCS 2705 hall effect current sensor and a LED panel.

Fig. 10a shows the experimental waveforms of input voltage and input current for rated lamp load power with the fuzzy-tuned PI voltage controller and the hysteresis current controller for LED driver. The input power factor and input current THD are measured with the power quality analyzer shown in Fig. 10b. Based on this Figure, the input power factor is 0.9992 and the input current THD is 1.753%.

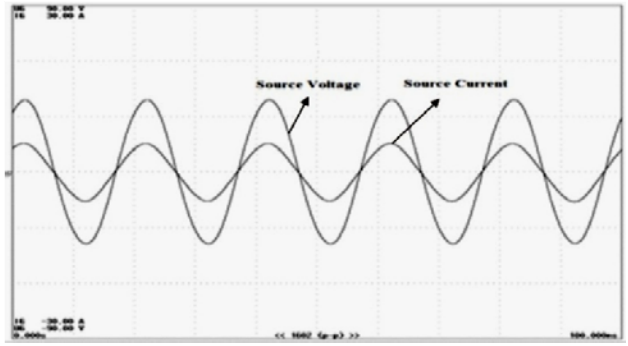

Fig. 10a. Experimental input voltage and input current waveforms at rated power with fuzzy-tuned PI voltage controller and hysteresis current controller for LED driver.

	Element 1	Element 2	Element 3	Element 4	Element 5	Element 6
Urms [V]	28.05	48.03	0.00	0.00	0.00	0.000
Irms [A]	3.9890	1.9421	0.0000	0.0000	0.0000	0.0000
P [W]	112.56	93.43	-0.00	0.0000k	0.0000k	0.00
S [VA]	112.51	100.45	0.00	0.0000k	0.0000k	0.00
Q [var]	0.00	-58.81	0.00	0.0000k	0.0000k	0.00
λ [ ]	0.9992	0.8107	Error	Error	Error	Error
S [VA]	112.51	100.45	0.00	0.0000k	0.0000k	0.00
Uthd [%]	0.409	1.189	0.0000	0.0000	0.0000	0.0000
Ithd [%]	1.753	1.185	0.0000	0.0000	0.0000	0.0000

Fig. 10b. Power quality measurements in element 1 for rated lamp load power with fuzzy-tuned PI voltage controller and hysteresis current controller for LED driver.

Fig. 10c shows the experimental waveforms of input voltage and input current for 25% of lamp load power with the fuzzy-tuned PI voltage controller and the hysteresis current controller for LED driver. The input power factor and input current THD are measured with the power quality analyzer shown in Fig. 10d. Based on this Figure, the input power factor is 0.9981 and the THD is 3.275%.

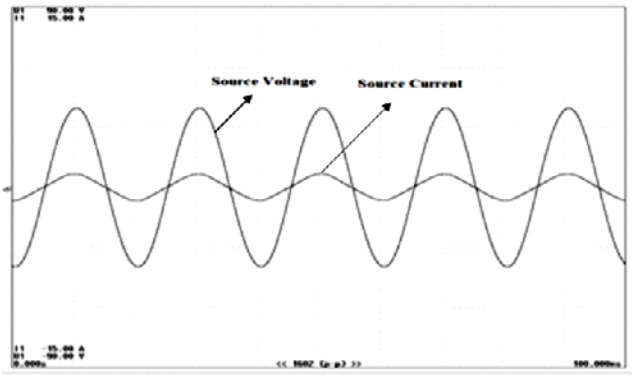

Fig. 10c. Experimental input voltage and input current waveforms at 25% of load power with fuzzy-tuned PI voltage controller and hysteresis current controller for LED driver.

	Element 1	Element 2	Element 3	Element 4	Element 5	Element 6
Urms [V]	28.09	48.09	0.00	0.00	0.00	0.000
Irms [A]	0.9932	0.4692	0.0000	0.0000	0.0000	0.0000
P [W]	27.68	22.77	-0.00	-0.0000k	-0.0000k	-0.00
S [VA]	27.55	28.09	0.00	0.0000k	0.0000k	0.00
Q [var]	0.00	-16.45	0.00	0.0000k	0.0000k	0.00
λ [ ]	0.9981	0.8106	Error	Error	Error	Error
S [VA]	27.55	28.09	0.00	0.0000k	0.0000k	0.00
Uthd [%]	0.909	0.330	0.0000	0.0000	0.0000	0.0000
Ithd [%]	3.275	0.330	0.0000	0.0000	0.0000	0.0000

Fig. 10d. Power quality measurements in element 1 for 25% of lamp load power with fuzzy-tuned PI voltage controller and hysteresis current controller for LED driver.

6. Comparative analysis of various controllers of proposed LED driver

Fig. 11a shows the simulation results of the input current total harmonic distortion comparison curve for PI, Fuzzy and Fuzzy-tuned PI along with the hysteresis current controller for LED driver. The proposed fuzzy-tuned PI controller-based single-phase AC-DC three-level LED driver provides better results compared with the PI and fuzzy voltage controller. The input current THD of the fuzzy-tuned PI voltage controller and the hysteresis current controller is 1.24% for three level LED driver. This value is very much lower than the IEEE-516 standard and IEC-61000-3-2.

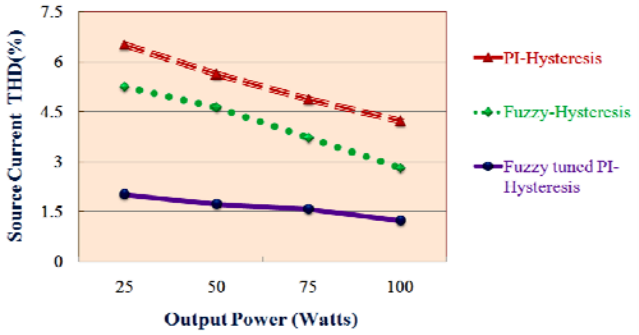

Fig. 11a. Simulation result with comparison of input current THD value for LED driver.

Fig. 11b shows the simulation results of the input power factor comparison curve for PI, fuzzy and fuzzy-tuned PI along with the hysteresis current controller for LED driver. The proposed fuzzy-tuned PI controller-based single-phase AC-DC three-level LED driver provides better results compared with the PI and fuzzy voltage controller. The input power factor of the fuzzy-tuned PI voltage controller and the hysteresis current controller is 1, which is close to unity for wide variations of lamp load power for three level LED driver.

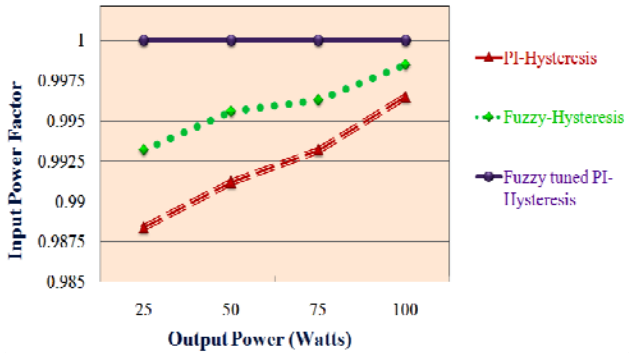

Fig. 11b. Simulation result with comparison of input power factor value for LED drive.

Fig. 11c shows the experimental result with a comparison of the input current THD value. The simulation results of the THD values of the fuzzy-tuned PI voltage controller and the hysteresis current controller for LED driver is 1.24%. The input current THD experimental result of the fuzzy-tuned PI with HCC for LED driver is 1.753%. This value is very much lower than the IEEE-516 standard and IEC-61000-3-2.

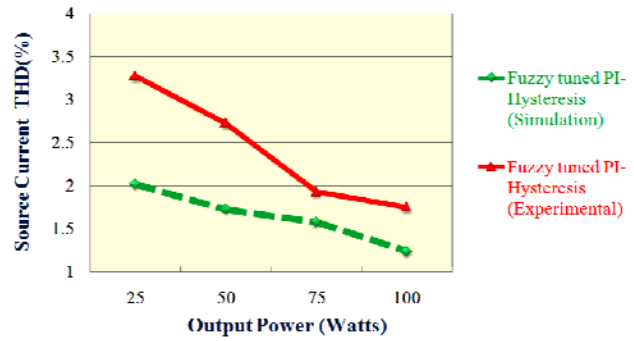

Fig. 11c. Experimental result with comparison of input current THD value for LED driver.

Fig. 11d shows the experimental result with a comparison of the input power factor. The input power factor of the fuzzy-tuned PI voltage controller and the hysteresis current controller for LED driver under simulation result is 1. The input power factor of the experimental result with the fuzzy-tuned PI voltage controller and the hysteresis current controller for LED driver is 0.9992.

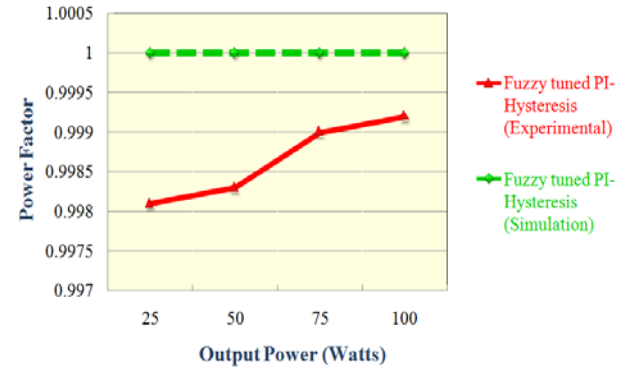

Fig. 11d. Experimental result with comparison of input power factor for LED driver.

7. Comparative analysis of conventional boost converter with proposed LED driver

The performance of the conventional boost LED driver and proposed LED drive in terms of the obtained input current THD and input PF at the supply mains with output power is evaluated as shown in Fig.12a and 12b respectively. Fuzzy tuned PI voltage controller and hysteresis current controller are implemented both LED drive. As shown theses figures, a very low input current harmonics and high input power factor are achieved for the proposed LED drive configuration.

.

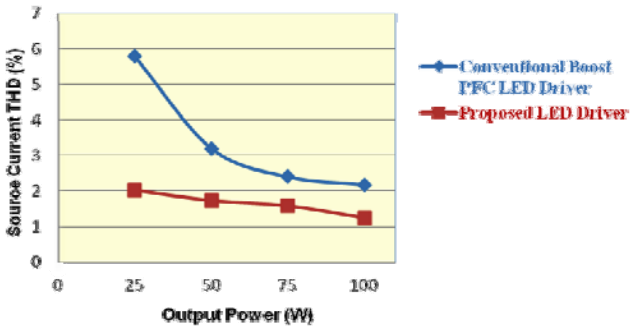

Fig. 12a. Comparison of input current THD for conventional boost and proposed LED drive.

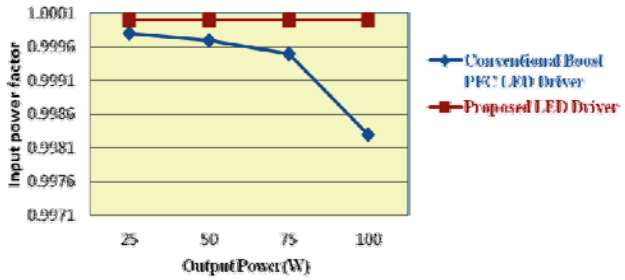

Fig. 12b. Comparison of input power factor for conventional boost and proposed LED drive.

8. Conclusion

This paper dealt with the simulation and implementation of closed-loop controllers for a single-phase AC-DC three-level LED driver for power quality enhancement in input AC supply side. The fuzzy-tuned PI voltage controller and the hysteresis current controller were implemented in a FPGA-based hardware platform for three level LED driver. The comparison revealed that the fuzzy-tuned PI voltage controller with the hysteresis current controller for three level LED driver showed better performance, with reduced input current THD of 1.24% in the simulation and 1.753% in the experiment, along with a input power factor close to unity without any source side LC filter.

References

[1] H. J. Chiu, S. J. Cheng, IEEE Transaction on Industrial Electronics, **5,** 2751(2007).

[2] H. Cho, O. K. Kwon, IEEE Trans. Consum. Electron., **4,** 2054 (2010).

[3] C. S. Moo, Y. J. Chen, W. C. Yang, IEEE Transaction Power Electronics, **11,** 4613 (2012).

[4] T. Hsieh, B. D. Liu, J. F. Wu, C. L. Fang, H. H. Tsai, Y. Z. Juang , IEEE Transactions on Power Electronics, **12,** 4562 (2012).

[5] B. Lee, H. Kim, C. Rim, IEEE Transactions on Power Electronics, **26,** 36941 (2011).

[6] N. Chen, H. S. H. Chung, IEEE Transactions on Power Electronics, **5,** 2551 (2013).

[7] O. Faruk Farsakoglu, I. Atik, J. Optoelectron. Adv. M., **17,** 277 (2015).

[8] An Tang,Yongtao Zhao, Haoming Zhang, Tao Ma, Fengxiang Shao, Hongsong Zhang , Optoelectron. Adv. Mat. **9,** 20 (2015).

[9] J. Liu, H. Yang, P. Jiang, M. Yu, Y. Huang, J. Yang, J. Optoelectron. Adv. M., **17,** 62 (2015).

[10] Wentao Zhang, Peicong Zhang, Junfeng Li, Kehui Qiu, Optoelectron. Adv. Mat. **8,** 37 (2014).

[11] Luqiao Yin, Jinlong Zhang, Yang Bai, Weiqiao Yang, Jianhua Zhang, Optoelectron. Adv. Mat, **8,** 427 (2014).

[12] O. F. Farsakoglu, H. Y. Hasirci, J. Optoelectron. Adv. M, **17,** 816 (2015).

[13] M. M. Jovanovic, D. E. Crow, IEEE Trans. Ind. Applicat., **33,** 551 (1997).

[14] R. Redl, Proc. IEEE Appl. Power Electron. Conf. (APEC), 454 (1998).

[15] A.R. Prasad, P. D. Ziogas, S. Manias, IEEE Trans. Ind. Electron, **37,** 521 (1990).

[16] Limits for Harmonic Current Emissions (Equipment Input Current <16A per Phase), IEC 1000/3/2 Int. Std., (1995).

[17] IEEE Industry Applications Soc. Power Engineering Soc., (1993).

[18] B. Singh, B. N. Singh, A. Chandra, K. Al-Haddad, A. Pandey, D. P. Kothari, IEEE Trans. on Industrial Electronics, **50,** 962 (2003).

[19] J.C. Crebier, B. Revol, J. P. Ferrieux, IEEE Trans. on Industrial Electronics, **52,** 36 (2005).

[20] S. Moon, L. Corradini, D. Maksimovic, IEEE Trans. on Power Electronics, **26,** 3006 (2011).

[21] M.Chen, J. Sun, IEEE Trans. on Power Electronics, **21,** 338 (2006).

[22] H.C. Chen, H. Y. Li, R. S. Yang, IEEE Trans. on Power Electronics, **24,** 1428 (2009).

[23] H.C. Chang, C. M. Liaw, IEEE Trans. on Industrial Electronics, **58,** 1763 (2011).

[24] J.Y. Chai, Y. H. Ho, Y. C. Chang, C. M. Liaw, IEEE Trans. on Industrial Electronics, **55,** 2576 (2008).

[25] L.S. Yang, T. J. Liang, H. C. Lee, J. F. Chen, IEEE Trans. on Industrial Electronics, **58,** 4196 (2011).

[26] W. Li, X. He, IEEE Trans.on Industrial Electronics, **58,** 1239 (2011).

[27] A.Shahin, M. Hinaje, J. P. Martin, S. Pierfederici, S.Rael, B. Davat, IEEE Trans. on Industrial Electronics, **57,** 3944 (2010).

[28] M. H. Todorovic, L. Palma, P. N. Enjeti, IEEE Trans.on Industrial Electronics, **55,** 1247 (2008).

[29] J.M. Kwon, B. H. Kwon, K. H. Nam, IEEE Trans. on Power Electronics, **23,** 2319 (2008).

[30] V. Yaramasu, B. Wu, Energy Conversion Congress and Exposition (ECCE), 561 (2011).

[31] M. T. Zhang, Y. Jiang, F. C. Lee, M. M. Jovanovic, IEEE APEC **95,** 434 (1995).

[32] R. Greul, S. D. Round, J. W. Kolar, IEEE Trans. on Power Electronics, **21,** 1637 (2006).

[33] B.R. Lin, H. H. Lu, IEEE Trans. on Aerospace and Electronic Systems, **36,** 189 (2000).

[34] B.R. Lin, H. H. Lu, IEEE Trans. on Industrial Electronics, **47,** 245 (2000).

[35] Hung-Chi Chen, Jhen-Yu Liao, IEEE Transactions on Industrial Electronics, **61,** (2014).

[36] M. Rajesh, B. Singh, IET Power Electronics, **7,** 1499 (2014).

[37] D. Gonzaloz Lambar, Javier S. Zuniga, A. Rodriguez Alonso, M. Rodriguez Gonzaloz, M. M. Hernando, IEEE Trans. on Power Electronics, **24**, 2032 (2009).

[38] Fanghua Zhang, Jianjun Ni, Yijie Yu, IEEE Trans. on Power Electronics, **28**, 4831 (2013).

[39] Woo-Jun Cha, Yong-Won Cho, Jung-Min Kwon, Bong-Hwan Kwon, Journal of Display Technology, **10**, 407 (2014).

[40] Peng Fang, Yan-Fei Liu, Parensh C.Sen, IEEE Journal of Emerging and selected topics in power electronics, **3**, 654 (2015)

[41] N. Senthil Kumar, V. Sadasivam, H. M. Asan Sukriya, Electric Power Components and Systems, **36,** 680 (2008).

[42] Prema Kannan, Senthil Kumar Natarajan, Subhransu Sekhar Dash, Mathematics problems in Engineering, Hindawi Publishing Corporation, Article ID 590861, (2013).

[43] A. Kessal, L. Rahmani, M. Mostefai, J. Gaubert, Electronics and Electrical Engineering – Kaunes: Technologija, **2**, 67 (2012).

[44] Kasinathan Pounraj, Rajasekaran Vairamani, Selvaperumal Sundramoorthy, IET Power Electronics, **5**, 843 (2013)

[45] H. C. Lee., IEEE Transactions on Fuzzy Systems, **19,** 265 (2011).

[46] Y. P. Pan, J. E. Meng, D. P. Huang, Q. R. Wang., IEEE Transactions on Fuzzy Systems,**19,** 807 (2011)

[47] Manjun Cai, Yue Wang, IEEE Transactions Ninth International Conference on Natural Computation (ICNC) on (2013).

[48] Sima Seidi Khorramabadi, Alireza Bakhshai, IEEE Transactions on smart grid, **6,** 92 (2015).

[49] A.Balestroni, A. Landi, L. Sani, IEEE Trans. Ind. Applications, **38,** 406 (2002).

*Corresponding author: jgvadivel@gmail.com,